

# Relation between the eigenfrequencies of Bogoliubov excitations of Bose-Einstein condensates and the eigenvalues of the Jacobian in a time-dependent variational approach

Manuel Kreibich, Jörg Main, and Günter Wunner

*1. Institut für Theoretische Physik, Universität Stuttgart, 70550 Stuttgart, Germany*

(Received 22 February 2012; published 6 July 2012)

We study the relation between the eigenfrequencies of the Bogoliubov excitations of Bose-Einstein condensates and the eigenvalues of the Jacobian stability matrix in a variational approach that maps the Gross-Pitaevskii equation to a system of equations of motion for the variational parameters. We do this for Bose-Einstein condensates with attractive contact interaction in an external trap and for a simple model of a self-trapped Bose-Einstein condensate with attractive  $1/r$  interaction. The stationary solutions of the Gross-Pitaevskii equation and Bogoliubov excitations are calculated using a finite-difference scheme. The Bogoliubov spectra of the ground and excited state of the self-trapped monopolar condensate exhibit a Rydberg-like structure, which can be explained by means of a quantum-defect theory. On the variational side, we treat the problem using an ansatz of time-dependent coupled Gaussian functions combined with spherical harmonics. We first apply this ansatz to a condensate in an external trap without long-range interaction and calculate the excitation spectrum with the help of the time-dependent variational principle. Comparing with the full-numerical results, we find good agreement for the eigenfrequencies of the lowest excitation modes with arbitrary angular momenta. The variational method is then applied to calculate the excitations of the self-trapped monopolar condensates and the eigenfrequencies of the excitation modes are compared.

DOI: [10.1103/PhysRevA.86.013608](https://doi.org/10.1103/PhysRevA.86.013608)

PACS number(s): 03.75.Kk, 67.85.De

## I. INTRODUCTION

In the quantum-mechanical description of the ground states of Bose-Einstein condensates in the framework of the Gross-Pitaevskii equation, the frequencies of elementary excitations of the condensates are obtained by solving the Bogoliubov–de Gennes equations. In an alternative description, a variational approach with coupled Gaussian functions has recently been proposed by Rau *et al.* [1,2] that maps the Gross-Pitaevskii equation to a dynamical system for the variational parameters that can be analyzed using the familiar tools of classical nonlinear dynamics. Ground states correspond to the fixed points of the dynamical system and their stability properties follow from the eigenvalues of the Jacobian at the fixed points. In this paper we shall investigate the question of whether or not there is a relation between the eigenvalues of the Jacobian and the eigenfrequencies of the quantum-mechanical Bogoliubov excitations and if so, to what extent the eigenvalues of the Jacobian can reproduce the frequencies of these excitations.

The realization of a Bose-Einstein condensate (BEC) with  $^{52}\text{Cr}$  atoms [3] marked the beginning of experimental investigations of BECs with long-range interactions. The anisotropic dipole-dipole interaction caused by the large magnetic moment of the  $^{52}\text{Cr}$  atoms influences the properties of the quantum gas [4] and is responsible for new phenomena such as a roton-maxon spectrum [5], structured ground states [6,7], and angular collapse [8]. Recently a condensate of  $^{164}\text{Dy}$  atoms with an even larger magnetic moment was created [9,10] and BECs of other lanthanides with a strong dipole-dipole interaction should be possible [11].

A model of a BEC with a different long-range interaction was proposed by O'Dell *et al.* [12]. In contrast to the dipolar interaction, this interaction is monopolar, i.e., gravitylike with an attractive  $1/r$  potential. Although it will be difficult to realize this model experimentally, BECs with monopolar long-range interaction are worth investigating in their own right since

they exhibit the phenomenon of self-trapping [12], i.e., the existence of a stable condensate without an additional external trap. Furthermore, the isotropic character of the interaction renders numerical investigations easier than in the anisotropic case and therefore BECs with monopolar interaction can serve as model systems for the treatment of condensates with long-range interactions to test new approaches and techniques.

The stationary states of self-trapped monopolar condensates have been calculated in the Thomas-Fermi regime and with the variational ansatz of a single Gaussian function [12], full numerically [13], and with an ansatz of coupled Gaussian functions [1,2]. Several aspects of the excitation spectrum have also been investigated [2,14,15], but a comprehensive study is still lacking. In this paper we will solve the Bogoliubov–de Gennes equations and reveal a Rydberg-like structure in the numerically exact Bogoliubov spectra, similar to the spectra of alkali metals.

The full-numerical calculations are very accurate if, depending on the method, the grid size, number of basis functions, etc., are chosen carefully, but may become computationally very expensive. As an alternative we pursue a variational ansatz with coupled Gaussian functions. Single Gaussian functions have been used in the literature to obtain qualitative results for BECs (e.g., in Ref. [12,16]). The ansatz can be extended to time-dependent coupled Gaussian functions [17,18] and it was demonstrated [1,2] that the method can quantitatively reproduce the properties of the stationary solutions of the Gross-Pitaevskii equation with both monopolar and dipolar long-range interactions. However, as we discuss below, the ansatz with coupled Gaussian functions can only describe excitations with a maximum angular momentum of  $l = 2$ . Several extensions of a Gaussian ansatz have been considered in the literature, e.g., Gaussian functions with Hermite or Laguerre polynomials [6,19,20] or sines and cosines [21]; however, these methods allow for no systematic improvement

of the ansatz, which is the case for the variational method we present in this paper.

Our variational ansatz is based on a combination of coupled Gaussian functions with spherical harmonics and can describe excitations with arbitrary angular momenta in radially symmetric systems. The power of the method will be demonstrated by applying it to BECs without and with monopolar long-range interaction.

The paper is organized as follows. In Sec. II we give the basic equations and describe our numerical method for calculating the stationary states and excitations of self-trapped monopolar condensates. We show that the Bogoliubov spectra can be nicely analyzed in terms of quantum-defect theory. Our variational ansatz with time-dependent coupled Gaussian functions combined with spherical harmonics is described in Sec. III and the equations of motion for the Gaussian parameters are derived. The method is applied to BECs without and with the monopolar long-range interaction. In Sec. IV we summarize and give an outlook for future work.

## II. FULL-NUMERICAL TREATMENT OF THE SELF-TRAPPED MONOPOLAR CONDENSATE

The time-dependent Gross-Pitaevskii equation (GPE) for the self-trapped condensate with short-range contact interaction and long-range monopolar interaction reads

$$i \frac{\partial \psi}{\partial t}(\mathbf{r}, t) = \left[ -\Delta + 8\pi a |\psi(\mathbf{r}, t)|^2 - 2 \int d^3 r' \frac{|\psi(\mathbf{r}', t)|^2}{|\mathbf{r} - \mathbf{r}'|} \right] \psi(\mathbf{r}, t), \quad (1)$$

where  $a$  denotes the  $s$ -wave scattering length. Since we will concentrate on the case of self-trapping, the external potential has been omitted. All variables in Eq. (1) are given in the natural units introduced in Ref. [13]: Lengths are measured in units of  $a_u = \hbar^2/mu$ , energies are measured in units of  $E_u = u/2a_u$ , and time is measured in units of  $t_u = \hbar/E_u$ . The quantity  $u$  is the coupling constant of the monopolar interaction defined in Ref. [12] and depends on the intensity and wave number of the laser and the polarizability of the atoms.

Equation (1) represents the GPE for the fictitious one-boson problem. One can make use of the scaling property of Ref. [13] to scale all quantities to an  $N$ -boson system:

$$(\mathbf{r}, a, t, \psi) \rightarrow (N\mathbf{r}, N^2a, N^2t, N^{-3/2}\psi). \quad (2)$$

The scaled dimensionless units are used throughout this work and in all figures whenever considering monopolar condensates. In these units the only remaining parameter is the scattering length  $a$  [13]. The stationary GPE can be obtained by substituting  $\psi(\mathbf{r}, t) = \psi(\mathbf{r}) \exp(-i\mu t)$ , with the chemical potential  $\mu$ , in the time-dependent GPE (1), which leads to

$$\mu \psi(\mathbf{r}) = \left[ -\Delta + 8\pi a |\psi(\mathbf{r})|^2 - 2 \int d^3 r' \frac{|\psi(\mathbf{r}')|^2}{|\mathbf{r} - \mathbf{r}'|} \right] \psi(\mathbf{r}). \quad (3)$$

### A. Calculation of stationary solutions

For a numerical treatment of the stationary GPE (3) it is convenient to convert the integro-differential equation into two coupled differential equations. This can be achieved by defining the mean-field potential

$$\phi(\mathbf{r}) = -2 \int d^3 r' \frac{|\psi(\mathbf{r}')|^2}{|\mathbf{r} - \mathbf{r}'|}. \quad (4)$$

Since we search for radially symmetric stationary solutions we assume the wave function and the mean-field potential to depend only on the radial coordinate:  $\psi(\mathbf{r}) = \psi(r)$  and  $\phi(\mathbf{r}) = \phi(r)$ . Letting the Laplacian in spherical coordinates act on Eq. (4), one obtains the two one-dimensional nonlinear coupled differential equations

$$\left( -\frac{d^2}{dr^2} - \frac{2}{r} \frac{d}{dr} + 8\pi a |\psi(r)|^2 + \phi(r) \right) \psi(r) = \mu \psi(r), \quad (5a)$$

$$\left( \frac{d^2}{dr^2} + \frac{2}{r} \frac{d}{dr} \right) \phi(r) - 8\pi |\psi(r)|^2 = 0. \quad (5b)$$

The system of equations (5) can be solved numerically in different ways. Since it is a one-dimensional problem, one can integrate the equations using a Runge-Kutta algorithm from  $r = 0$  to a sufficiently large value  $r_{\max}$  with appropriately chosen initial conditions for  $\psi(0)$ ,  $\psi'(0)$ ,  $\phi(0)$ , and  $\phi'(0)$  [13,15,22]. Their values must be varied until the wave function converges towards zero at  $r = r_{\max}$ . With this method the ground and excited states can be calculated efficiently. However, to obtain a normalized solution  $\psi(r)$  the wave function, scattering length, and mean-field energy must be rescaled. Thus it is difficult to obtain a solution for a given fixed value of the scattering length. Additionally, it is not easy to calculate the Bogoliubov spectrum of the system with this method since the solutions of the Bogoliubov–de Gennes (BDG) equations have large extensions and a very big value of  $r_{\max}$  has to be chosen. For example, to calculate 20 eigenvalues for an angular momentum of  $l = 6$ ,  $r_{\max}$  needs to be larger than 1000. In this case machine precision in the Runge-Kutta method is not sufficient to obtain converged solutions, leaving this method useless for higher modes. In Refs. [2,15] only the three lowest  $l = 0$  modes could be calculated.

Another method is the imaginary time evolution [replacement  $t \rightarrow t = i\tau$  in Eq. (1)] of an initial wave function on a grid. As time evolves the wave function converges to the ground state. This method is useful to find the ground state or a metastable state of a system. However, a collectively excited state, as we consider below, cannot be obtained by imaginary time evolution.

To avoid these disadvantages, we use the finite-difference method to solve the stationary GPE (5): The wave function and the mean-field potential are discretized on a grid and all derivatives are replaced by their finite-difference approximation. To arrive at a closed system of algebraic equations that can be solved by a nonlinear root search one needs appropriate boundary conditions  $\psi'(0) = 0$  and  $\phi'(0) = 0$  to ensure that the functions are differentiable at the origin and  $\psi(r_{\max}) = 0$  to obtain a normalizable wave function. The fourth boundary condition can be obtained by looking

at the asymptotic behavior of the mean-field potential (4). Approximating  $1/|\mathbf{r} - \mathbf{r}'| \approx 1/r$  for  $r \gg r'$  and assuming a normalized wave function  $\psi$ , one obtains from Eq. (4)  $\phi(r) \approx -2/r$ . The fourth boundary condition is therefore set to be  $\phi(r_{\max}) = -2/r_{\max}$ .

We perform the nonlinear root search using the Powell hybrid method [23]. In addition to the equations originating from the finite-difference scheme, the normalization condition has to be included, as well as the chemical potential as a parameter to be determined by the root search.

### B. Bogoliubov–de Gennes equations

The stability and elementary excitations of a self-trapped monopolar condensate have already been analyzed in the literature: the lowest monopole and quadrupole oscillation analytically and numerically [14], the first monopole modes [22], and the lowest monopole and quadrupole modes by means of a variational ansatz with coupled Gaussian functions [2]. However, to the best of our knowledge, a calculation of the Bogoliubov spectrum for arbitrary angular momenta and higher excitations does not yet exist.

To derive the BDG equations, one starts from the usual ansatz for a perturbation of a stationary state

$$\psi(\mathbf{r}, t) = \{\psi_0(\mathbf{r}) + \lambda[u(\mathbf{r})e^{-i\omega t} + v^*(\mathbf{r})e^{i\omega^* t}]\}e^{-i\mu t}, \quad (6)$$

where  $\omega$  is the frequency and  $\lambda$  is the amplitude of the perturbation ( $|\lambda| \ll 1$ ) and  $\mu$  is the chemical potential of the stationary solution  $\psi_0$  with corresponding mean-field potential  $\phi_0$ . Equation (6) is inserted into the time-dependent GPE (1), terms of second order in  $\lambda$  are neglected, and collecting terms evolving in time with  $\exp(-i\omega t)$  and  $\exp(i\omega^* t)$  yields the BDG equations

$$\omega u(\mathbf{r}) = [-\Delta - \mu + 16\pi a |\psi_0(\mathbf{r})|^2 + \phi_0(\mathbf{r})]u(\mathbf{r}) + 8\pi a [\psi_0(\mathbf{r})]^2 v(\mathbf{r}) + \psi_0(\mathbf{r})f(\mathbf{r}), \quad (7a)$$

$$-\omega v(\mathbf{r}) = [-\Delta - \mu + 16\pi a |\psi_0(\mathbf{r})|^2 + \phi_0(\mathbf{r})]v(\mathbf{r}) + 8\pi a [\psi_0^*(\mathbf{r})]^2 u(\mathbf{r}) + \psi_0^*(\mathbf{r})f(\mathbf{r}), \quad (7b)$$

with the auxiliary field (similar to the mean-field potential)

$$f(\mathbf{r}) = -2 \int d^3 r' \frac{\psi_0^*(\mathbf{r}')u(\mathbf{r}') + \psi_0(\mathbf{r}')v(\mathbf{r}')}{|\mathbf{r} - \mathbf{r}'|}. \quad (8)$$

The ansatz of Eq. (6) possesses a symmetry: The exchange of  $u(\mathbf{r}) \leftrightarrow v^*(\mathbf{r})$  and  $\omega \leftrightarrow -\omega^*$  leaves the ansatz invariant. Thus for each solution  $(u, v)$  and  $\omega$  of Eqs. (7),  $(v^*, u^*)$  with  $-\omega^*$  is another solution and both solutions represent the same physical motion. For that reason, only solutions with  $\text{Re } \omega \geq 0$  need to be considered. There are two solutions of Eqs. (7) that deserve special attention. If  $\psi_0$  is assumed to be real, then  $u(\mathbf{r}) = -v(\mathbf{r}) = \psi_0(\mathbf{r})$  is a solution of Eqs. (7) with the frequency  $\omega = 0$ . This represents the well-known gauge transformation of the condensate wave function  $\psi(\mathbf{r}) \rightarrow \psi(\mathbf{r}) \exp(i\phi)$  with a real phase  $\phi$ . This gauge mode does not describe a physical motion of the condensate and since it is always part of the Bogoliubov spectrum, we will not discuss it when presenting the results.

Furthermore, there always exist solutions of the BDG equations with frequencies identical to the trapping frequencies [24]. These modes represent the center-of-mass oscillations of

the condensate along the three space directions with angular momentum  $l = 1$ . In the case of the self-trapped monopolar condensate, there are no external traps and therefore the frequencies are  $\omega = 0$ , which corresponds to a constant displacement of the condensate.

Since the wave function  $\psi_0$  and the mean-field potential  $\phi_0$  are radially symmetric, we can separate the solutions  $u$  and  $v$  by means of spherical harmonics

$$u_{nlm}(\mathbf{r}) = Y_{lm}(\theta, \phi)u_{nl}(r), \quad (9a)$$

$$v_{nlm}(\mathbf{r}) = Y_{lm}(\theta, \phi)v_{nl}(r), \quad (9b)$$

with the radial (excitation) quantum number  $n$  and the usual angular momentum quantum numbers  $l$  and  $m$ . Using the multipole expansion of the integration kernel  $1/|\mathbf{r} - \mathbf{r}'|$  [see, e.g., Ref. [25] and Eq. (A29)], we can also express the auxiliary field (8) in the form  $f_{nlm}(\mathbf{r}) = Y_{lm}(\theta, \phi)f_{nl}(r)$  with ( $\psi_0$  and  $\phi_0$  are assumed to be real from now on)

$$f_{nl}(r) = \frac{-8\pi}{2l+1} \int_0^\infty dr' (r')^2 \frac{r_{<}^l}{r_{>}^{l+1}} \psi_0(r') [u_{nl}(r') + v_{nl}(r')], \quad (10)$$

where  $r_{<} = \min(r, r')$  and  $r_{>} = \max(r, r')$ , respectively. Inserting the Laplacian in spherical coordinates and using the separation (9), we finally obtain from Eqs. (7)

$$\omega_{nl}u_{nl}(r) = \left[ -\frac{d^2}{dr^2} - \frac{2}{r} \frac{d}{dr} + \frac{l(l+1)}{r^2} - \mu + 16\pi a \psi_0^2(r) + \phi_0(r) \right] u_{nl}(r) + 8\pi a \psi_0^2(r) v_{nl}(r) + \psi_0(r) f_{nl}(r), \quad (11a)$$

$$-\omega_{nl}v_{nl}(r) = \left[ -\frac{d^2}{dr^2} - \frac{2}{r} \frac{d}{dr} + \frac{l(l+1)}{r^2} - \mu + 16\pi a \psi_0^2(r) + \phi_0(r) \right] v_{nl}(r) + 8\pi a \psi_0^2(r) u_{nl}(r) + \psi_0(r) f_{nl}(r). \quad (11b)$$

We solve Eqs. (11) using the finite-difference method. After choosing a grid, approximating the derivatives by finite differences and replacing the integral in the auxiliary field  $f$  by an appropriate integration rule (we use the trapezoidal rule), Eqs. (11) turn into a matrix eigenvalue problem

$$\mathbf{M} \begin{pmatrix} u \\ v \end{pmatrix} = \omega \begin{pmatrix} u \\ v \end{pmatrix}. \quad (12)$$

The eigenvalues of the matrix  $\mathbf{M}$  can then be found by numerical diagonalization.

In actual calculations we found it advantageous to choose a nonequidistant grid since the solutions  $u$  and  $v$  can be highly oscillatory near the origin and at the same time extend to large values of  $r$ . We use partially equidistant grids, i.e., an equidistant grid with step size  $\Delta r_1$  in the interval  $[0, r_1]$ , another equidistant grid with a different  $\Delta r_2$  in the interval  $[r_1, r_2]$ , etc.

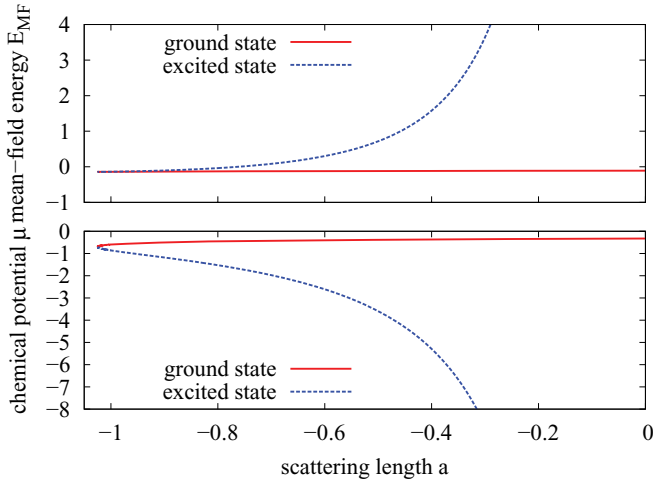


FIG. 1. (Color online) Mean-field energy  $E_{\text{MF}}$  and chemical potential  $\mu$  of the ground and excited state of a self-trapped monopolar condensate as functions of the scattering length  $a$ . For a scattering length lower than the critical value of  $a_{\text{crit}} \approx -1.025$  no stationary solution exists. At  $a = a_{\text{crit}}$  the two solutions emerge in a tangent bifurcation. For the ground state, both  $E_{\text{MF}}$  and  $\mu$  stay negative in the range of the scattering length considered. These quantities diverge for the excited state in the limit  $a \rightarrow 0$ .

### C. Results

Since the properties of the stationary solution have been discussed in detail in the literature [13,15,22], we give only a brief review. Our results coincide with those obtained using the outward integration method and thus for the stationary states both methods can be considered equally applicable. In Fig. 1 we plot the mean-field energy  $E_{\text{MF}}$  and the chemical potential  $\mu$  of the ground and excited state as a function of the scattering length  $a$ . Two solutions emerge in a tangent bifurcation at the critical scattering length  $a = a_{\text{crit}} \approx -1.025$ . At this point the mean-field energy, chemical potential, and wave functions of the ground and excited state merge. For  $a \rightarrow 0$  the mean-field energy and chemical potential of the excited state diverge, implying that this state does not exist for  $a \geq 0$ .

Using the method described in Sec. II B, we have calculated the Bogoliubov spectrum of the ground state. For the angular momenta from  $l = 0$  to 3, Fig. 2 shows the frequencies of the Bogoliubov excitations as a function of the scattering length  $a$ . The ground state is stable since its spectrum contains only real frequencies. It can be seen that as the scattering length is decreased toward its critical value the frequency of the lowest mode with  $l = 0$  at first slightly increases but then goes to zero at  $a \rightarrow a_{\text{crit}}$ , where the state vanishes. This mode is responsible for the collapse of the condensate. The lowest  $l = 1$  mode has the frequency  $\omega = 0$  and corresponds to the displacement of the center of mass of the condensate. This frequency remains constantly  $\omega = 0$  as the scattering length is varied and as already mentioned corresponds to the (vanishing) trapping frequency.

The results for the excited state are presented in Fig. 3. All frequencies merge with those of the ground-state modes at the critical scattering length. There exists one imaginary frequency for the angular momentum  $l = 0$ . Therefore the excited state is unstable with respect to this excitation, which leads to a

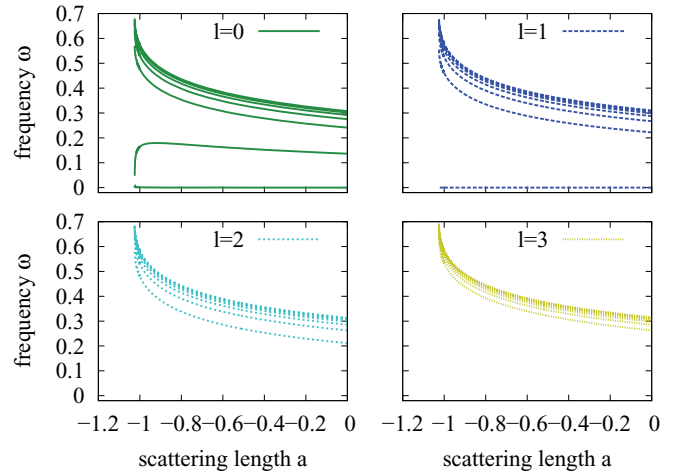


FIG. 2. (Color online) Frequencies of Bogoliubov excitations of the ground state in Fig. 1 for the angular momenta from  $l = 0$  to 3 as functions of the scattering length  $a$ . The seven lowest eigenvalues are shown for each angular momentum. The spectrum only contains real frequencies, i.e., the ground state is stable. The lowest mode for  $l = 0$  tends to zero as  $a \rightarrow a_{\text{crit}}$ , which leads to the collapse of the condensate. The lowest  $l = 1$  mode corresponds to a displacement of the center of mass of the condensate, while its shape remains unaffected. The frequency of this mode is exactly the trapping frequency [24], in this case  $\omega = 0$ . The frequencies of the other modes increase as the scattering length is decreased, finally merging with the modes of the excited state for  $a \rightarrow a_{\text{crit}}$  (see Fig. 3). Note that for fixed scattering length the distance between adjacent frequencies diminishes with growing radial quantum number, indicating the convergence of the frequencies to a (scattering-length-dependent) limit frequency.

collapse with  $l = 0$  symmetry. As for the ground state, the lowest mode with  $l = 1$  represents the displacement of the condensate and is constantly  $\omega = 0$ .

In Fig. 4 the Bogoliubov functions  $u$  and  $v$  are shown for the angular momentum  $l = 0$ . The lowest functions with  $n = 1$  and 2 are concentrated near the origin and have the same extension as the wave function of the stationary solution (see Fig. 6). For the higher modes the functions  $u$  extend further, which is a consequence of the missing external trapping potential.

### D. Quantum-defect analysis of the Bogoliubov spectrum

To prove that for given scattering length the frequencies of the Bogoliubov excitations converge to a limiting frequency we determined the 20 lowest modes for the angular momenta  $l = 0-6$ . As an example, Fig. 5 shows, for the scattering length  $a = -0.4$ , the Bogoliubov spectrum of the ground state. The convergence of the frequencies to a common limit, independently of  $l$ , is evident. The spectrum is reminiscent of Rydberg spectra known from alkali-metal atoms. Similar to the spectra of these atoms, the structure of the Bogoliubov spectra can be understood in terms of quantum-defect theory.

For large values of  $r$  the BDG equations (11) simplify due to the fact that the wave function decays exponentially and the mean-field potential converges to  $\phi_0(r) \approx -2/r$  (see Fig. 6). Setting  $\psi_0(r) \approx 0$  for  $r > r_c$ , all terms containing  $\psi_0$  can be

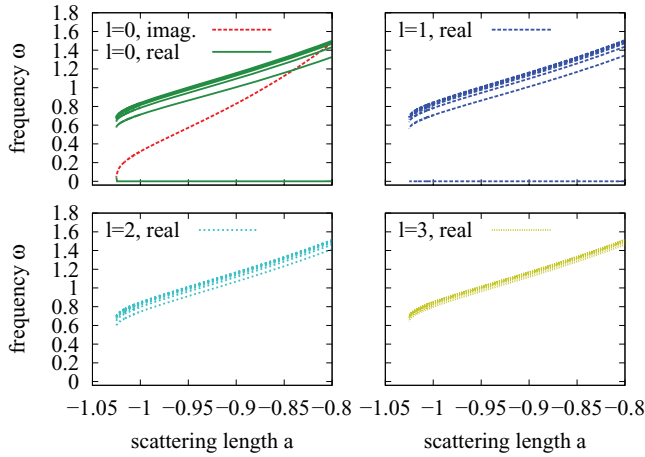


FIG. 3. (Color online) Same as Fig. 2, but for the excited state. There is one imaginary frequency for  $l = 0$ : The excited state is unstable with respect to small perturbations. As for the ground state, the lowest  $l = 1$  mode is  $\omega = 0$  and corresponds to a displacement of the center of mass of the condensate. Again, the frequencies of the stable modes apparently converge to a limit for fixed scattering length.

neglected in Eqs. (11) and  $\phi_0$  can be approximated by  $-2/r$ . This leads to the asymptotic form of the BDG equations

$$\omega_{nl} u_{nl}(r) = \left[ -\frac{d^2}{dr^2} - \frac{2}{r} \frac{d}{dr} + \frac{l(l+1)}{r^2} - \mu - \frac{2}{r} \right] u_{nl}(r), \quad (13a)$$

$$-\omega_{nl} v_{nl}(r) = \left[ -\frac{d^2}{dr^2} - \frac{2}{r} \frac{d}{dr} + \frac{l(l+1)}{r^2} - \mu - \frac{2}{r} \right] v_{nl}(r). \quad (13b)$$

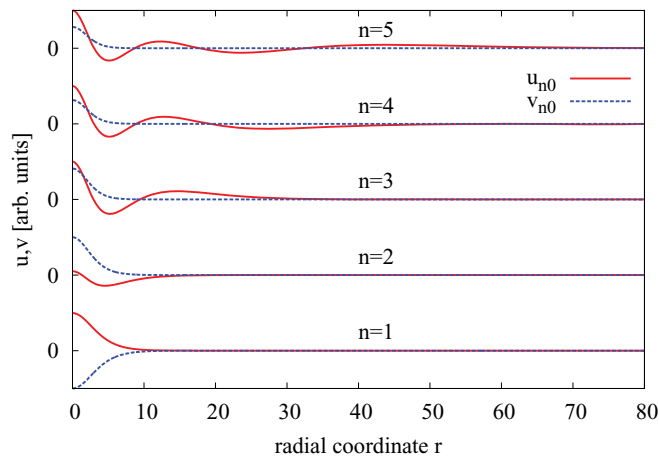


FIG. 4. (Color online) Bogoliubov functions  $u_{nl}(r)$  and  $v_{nl}(r)$  for the angular momentum  $l = 0$  and the radial quantum numbers  $n = 1, \dots, 5$ . The scattering length is  $a = -0.4$ . The mode with  $n = 1$  represents the gauge mode discussed in Sec. II B and the functions  $u_{10}(r)$  and  $v_{10}(r)$  are equal to the stationary solution  $\psi_0$ , except for the sign. The functions  $u_{n0}(r)$  have  $n - 1$  nodes, whereas all functions  $v_{n0}(r)$  show qualitatively the same behavior and are nodeless for all  $n$ . It can be seen that with growing radial quantum number the functions  $u_{n0}(r)$  extend to ever increasing values of  $r$ .

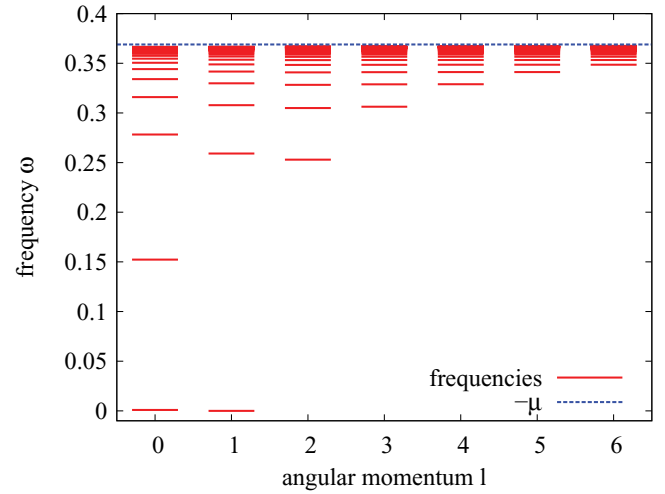


FIG. 5. (Color online) Frequencies of the Bogoliubov excitations of the ground state of a self-trapped monopolar BEC for a fixed scattering length  $a = -0.4$ , plotted for different values of the angular momentum. The dotted line gives the value of the chemical potential. Obviously, as shown in Figs. 2 and 3, the frequencies converge to a common limit, which is the chemical potential. The Bogoliubov spectrum can be described by a Rydberg formula with quantum defects.

Obviously in this limit  $u$  and  $v$  obey the same equation, namely, the Schrödinger equation of the Coulomb problem, except for the opposite sign of the eigenvalues. Therefore asymptotically only one equation of Eqs. (13) needs to be considered (which will be the one for  $u$ ). The scattering length enters into Eqs. (13) only indirectly via  $\mu = \mu(a)$ .

The approximations made are valid only if the function values of  $u$  and  $v$  are small for  $r < r_c$ . Especially for lower angular momenta, this is not the case. In the physics of alkali

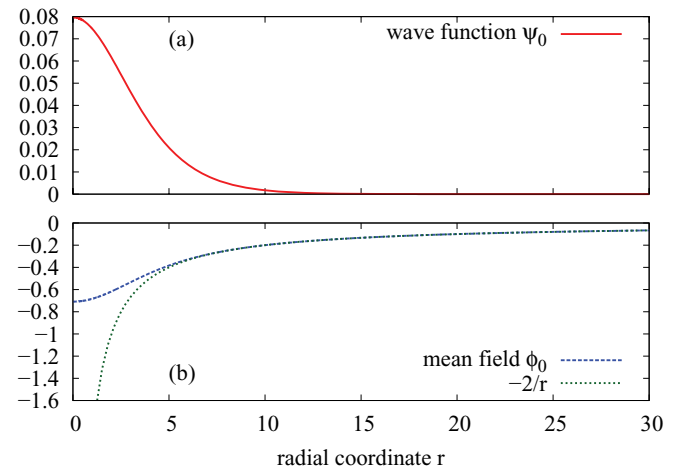


FIG. 6. (Color online) (a) Wave function  $\psi_0$  and (b) mean-field potential  $\phi_0$  for the ground state of a self-trapped monopolar condensate at a scattering length of  $a = -0.4$  as functions of the radial coordinate  $r$ . The wave function approaches zero exponentially, whereas the mean-field potential behaves like  $-2/r$  for large values of  $r$ . In this region, the wave function can be neglected and the mean-field potential replaced by its asymptotic form in the BDG equations.

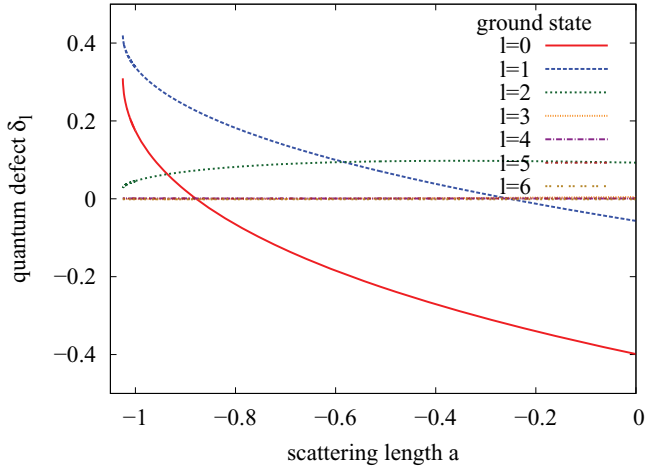


FIG. 7. (Color online) Calculated quantum defects  $\delta_l$  for the Bogoliubov spectrum of the ground state (Fig. 2) dependent on the scattering length  $a$  for different angular momenta  $l$ . The quantum defects for  $l = 0$  and 1 rise steeply and turn from negative to positive as the scattering length is decreased, while the quantum defect for  $l = 2$  shows only a weak dependence on the scattering length and drops close to the critical scattering length. As expected, for the higher angular momenta  $l > 2$  the quantum defects are close to zero.

metals a similar problem occurs: The valence electron far away from the nucleus experiences an attractive  $-1/r$  potential, which results from the shielding of the core electrons. Close to the nucleus, the core electrons and the true nuclear potential have to be considered. A similar situation happens here (cf. Fig. 6). To account for the deviation of the potential from the pure Coulomb potential at smaller values of the radial coordinate we can also introduce a quantum defect in the formula for the Rydberg series eigenvalues (see, e.g., Ref. [26]),

$$\omega_{nl} = -\mu - \frac{1}{(n+l+1-\delta_l)^2}, \quad (14)$$

where the quantum defects  $\delta_l$  depend on the angular momentum. The negative chemical potential is the limit of the frequencies for  $n \rightarrow \infty$ . The quantum defects can be obtained by least-squares fits of the Bogoliubov frequencies  $\omega_{nl}$  to Eq. (14). They converge to constant values for large  $n$ . Since Eq. (14) strictly holds only in this limit, in the fits it can be necessary to neglect the lowest frequencies.

For growing angular momentum, the repulsive effective potential  $l(l+1)/r^2$  becomes stronger and this centrifugal barrier ensures that the absolute values of the functions  $u$  and  $v$  decrease close to the origin  $r = 0$ . This leads to a smaller quantum defect  $\delta_l$  since the approximation made in deriving Eqs. (13) becomes valid at smaller values of  $r$ . In accordance with the quantum defects in alkali metals [26], the quantum defects therefore will tend to zero for higher angular momenta.

In Fig. 7 we present the quantum defects calculated for the Bogoliubov excitations of the ground state. Obviously the quantum defects for  $l = 0$  and 1 show a strong dependence on the scattering length, while for  $l \geq 2$  they are almost constant and in particular close to zero for  $l > 2$ . Equation (14) reproduces the frequencies of the Bogoliubov excitations of the ground state for all modes with an absolute error of less than

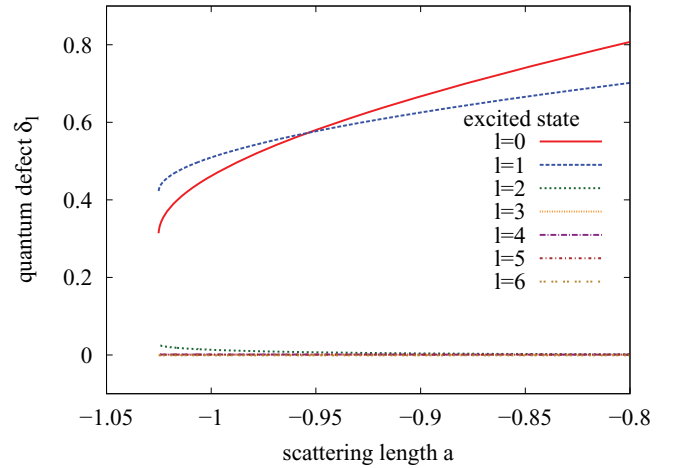


FIG. 8. (Color online) Same as Fig. 7, but for the excited state. Since the Bogoliubov spectra of the ground and excited states merge at the critical scattering length, the same holds for the quantum defects. The quantum defects  $\delta_0$  and  $\delta_1$  grow as the scattering length is increased, whereas  $\delta_2$  drops and tends to zero. As in the case of the ground state, the quantum defects for  $l > 2$  are close to zero.

$10^{-3}$ , except for the two lowest  $l = 0$  modes and the lowest  $l = 1$  mode. The quantum-defect analysis for the Bogoliubov excitations of the excited state is presented in Fig. 8. The quantitative statements made for the excitations of the ground state also hold for this state. The only difference is that the quantum defect for  $l = 2$  tends to zero as the scattering length is increased.

Thus by means of quantum-defect analysis we have been able to explain the Rydberg-like structure of the Bogoliubov spectra of the ground and excited states of self-trapped monopolar BECs and could confirm that the negative chemical potential is the limit of the frequencies for all angular momenta.

### III. VARIATIONAL APPROACH WITH GAUSSIAN FUNCTIONS AND SPHERICAL HARMONICS

We now turn our attention to variational calculations. The simplest ansatz with a single Gaussian function centered at the origin was used by Pérez-García *et al.* [16] to determine monopolar and quadrupolar modes of BECs without long-range interactions. The ansatz was improved by using coupled Gaussian functions [17,18] and it was shown [1,2] that this method is capable of reproducing accurately the stationary states even of BECs with long-range interactions, calculated numerically. The ansatz employed to determine the stationary solution of a radially symmetric condensate was

$$\psi = \sum_{k=1}^N e^{-A_r^k r^2 - \gamma^k}, \quad (15)$$

where the complex quantities  $A_r^k$  and  $\gamma^k$  are the widths and the amplitudes, respectively, of each Gaussian function. The above ansatz can only describe monopolar excitation modes since the wave function  $\psi$  is independent of the angular coordinates  $\theta$  and  $\phi$ . If one chooses the widths differently for each space

direction,

$$\psi = \sum_{k=1}^N e^{-A_x^k x^2 - A_y^k y^2 - A_z^k z^2 - \gamma^k}, \quad (16)$$

the width of a condensate can oscillate independently in each direction, which represents quadrupolar oscillations.

A generalization of Eqs. (15) and (16), which includes general square and linear terms in the exponentials, is [17,18]

$$\psi = \sum_{k=1}^N g^k \equiv \sum_{k=1}^N \exp[-\mathbf{r}^T \mathbf{A}^k \mathbf{r} - (\mathbf{p}^k)^T \mathbf{r} - \gamma^k], \quad (17)$$

with complex symmetric matrices  $\mathbf{A}^k$ , complex vectors  $\mathbf{p}^k$ , and complex numbers  $\gamma^k$ . This ansatz can describe excitation modes with angular momenta up to  $l = 2$ . To see this consider a small deviation  $\delta \mathbf{z}$  of the variational parameters from those of a stationary solution  $\mathbf{z}_0$  and Taylor expand the ansatz with coupled Gaussian functions (17) for the perturbed wave function  $\psi(\mathbf{z}_0 + \delta \mathbf{z})$  to first order in  $\delta \mathbf{z}$ ,

$$\begin{aligned} \delta \psi &= \delta \mathbf{z} \cdot \left. \frac{\partial \psi}{\partial \mathbf{z}} \right|_{\mathbf{z}=\mathbf{z}_0} \\ &= - \sum_{k=1}^N [\mathbf{r}^T \delta \mathbf{A}^k \mathbf{r} + (\delta \mathbf{p}^k)^T \mathbf{r} + \delta \gamma^k] g^k \Big|_{\mathbf{z}=\mathbf{z}_0}. \end{aligned} \quad (18)$$

Since only terms at most quadratic in  $x$ ,  $y$ , and  $z$  appear in front of the exponentials, these terms can be expressed by spherical harmonics with angular momenta  $l = 0, 1, 2$ , which proves our statement.

We apply an ansatz that is capable of describing excitations with, in principle, arbitrary angular momenta. Motivated by the separation in the BDG equations with spherical harmonics in Eq. (9), we directly include the spherical harmonics in an extended variational ansatz

$$\psi = \sum_{k=1}^N \left( 1 + \sum_{(l,m) \neq (0,0)} d_{lm}^k Y_{lm}(\theta, \phi) r^l \right) e^{-A_r^k r^2 - \gamma^k}. \quad (19)$$

The amplitudes  $d_{lm}^k$  account for additional angular momenta  $(l, m)$ . The sum over  $(l, m)$  may include arbitrary angular momenta, adjusted to the problem. For instance, if one wishes to calculate the linear perturbation of a specific angular momentum  $(l, m)$ , as we do below, the sum in Eq. (19) needs to include  $(l, m)$  and  $(l, -m)$  since the nonlinear terms in the GPE lead to a coupling of different angular momenta.

### A. Equations of motion and stability analysis

In order to carry out calculations with the extended variational ansatz (19) we need the equations of motion for the variational parameters. We use the approach of Ref. [1] based on the Dirac-Frankel-McLachlan time-dependent variational principle [27,28]. An arbitrary ansatz for the wave function is made  $\psi = \psi(\mathbf{z})$ , with the generally complex variational parameters  $\mathbf{z} = (z_1, \dots, z_M)$  for a system governed by the Schrödinger equation

$$i \dot{\psi} = \hat{H} \psi, \quad (20)$$

where the Hamiltonian  $\hat{H}$  may contain nonlinear terms in the wave function. The principle states that the norm of

the difference between the left- and the right-hand sides of Eq. (20),

$$I = \|i\dot{\psi}(t) - \hat{H}\psi(t)\|^2, \quad (21)$$

must be minimized. For a fixed time  $t$ ,  $\psi(t)$  is given and  $I$  is minimized by varying  $\phi(t)$ . After the minimization,  $\phi$  is set to  $\phi = \dot{\psi}$ . A necessary condition for the minimization of  $I$  is [15]

$$\mathbf{K} \dot{\mathbf{z}} = -i \mathbf{h}, \quad (22)$$

where the matrix  $\mathbf{K}$  and the vector  $\mathbf{h}$  are defined by

$$K_{ij} = \left\langle \frac{\partial \psi}{\partial z_i} \left| \frac{\partial \psi}{\partial z_j} \right. \right\rangle, \quad (23a)$$

$$h_i = \left\langle \frac{\partial \psi}{\partial z_i} \left| \hat{H} \psi \right. \right\rangle. \quad (23b)$$

Stationary solutions can then be found by requiring

$$\dot{z}_i = -i \sum_{j=1}^M (\mathbf{K}^{-1})_{ij} h_j = \begin{cases} i\mu & \text{for } z_i \equiv \gamma^k \\ 0 & \text{otherwise} \end{cases} \quad (24)$$

and searching for  $\mathbf{z}$  in a nonlinear root search.

The stability properties and linear oscillations of a stationary solution  $\mathbf{z}_0$  can be found by first changing from the complex  $M$ -dimensional vector  $\mathbf{z}$  to a real  $2M$ -dimensional vector  $\tilde{\mathbf{z}}$  containing the real and imaginary parts of the variational parameters and considering a small perturbation  $\tilde{\mathbf{z}}(t) = \tilde{\mathbf{z}}_0 + \delta \tilde{\mathbf{z}}(t)$ . Linearization of the equations of motion (22) yields the time dependence of the perturbation [1]

$$\delta \dot{\tilde{\mathbf{z}}}(t) = \mathbf{J} \delta \tilde{\mathbf{z}}(t) \quad (25)$$

with the Jacobian

$$J_{ij} = \frac{\partial \dot{\tilde{z}}_i}{\partial \tilde{z}_j} \quad (26)$$

evaluated at the fixed point  $\tilde{\mathbf{z}} = \tilde{\mathbf{z}}_0$ . The excitation modes of the stationary solutions are finally found by diagonalizing the Jacobian  $\mathbf{J}$ .

All integrals appearing in Eq. (22) with the ansatz (19) can be calculated analytically. The contact interaction leads to integrals over four spherical harmonics, which can be expressed in terms of Wigner 3- $j$  symbols. The contribution of long-range monopolar potential can be evaluated by inserting the multipole expansion for the monopolar integration kernel, which leads to Gaussian integrals. For further details of the calculations we refer to the Appendix.

### B. Test in a system without long-range interactions

As a first test we apply the extended variational ansatz (19) to a condensate in a radially symmetric trap with short-range scattering interaction. The GPE for this system reads

$$i \frac{\partial \psi}{\partial t}(\mathbf{r}, t) = [-\Delta + r^2 + 8\pi a |\psi(\mathbf{r}, t)|^2] \psi(\mathbf{r}, t). \quad (27)$$

Here units based on the trapping frequency  $\gamma = \omega/2$  and the harmonic-oscillator length  $a_0 = \sqrt{\hbar/m\omega}$  have been used. The scaled dimensionless scattering length  $a$  in Eq. (27) corresponds to  $Na/a_0$  in SI units, with the particle number  $N$ . These units will be used in all figures for the condensate

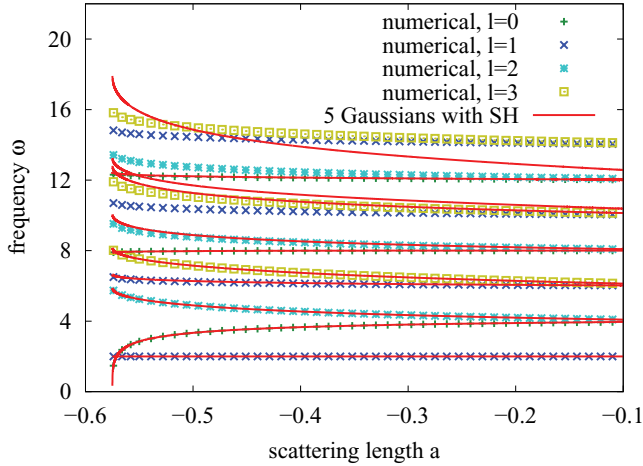


FIG. 9. (Color online) Comparison of the full-numerical Bogoliubov spectrum of a BEC with attractive contact interaction with the spectrum obtained from the variational ansatz with coupled Gaussian functions and spherical harmonics (SH). The variational ansatz has been used with five coupled Gaussian functions and spherical harmonics up to an angular momentum of  $l = 3$ . For the lowest modes we find excellent agreement. There are almost no deviations for frequencies  $\omega < 10$ . Just slightly above the critical scattering length small differences can be seen in the figure. For the higher modes, differences become larger and the variational ansatz can only qualitatively describe the Bogoliubov modes correctly.

without long-range interaction. The BDG equations are given in Eqs. (7) and (11), respectively, with all terms containing the mean-field potential  $\phi_0$  and the auxiliary field  $f$  omitted and the trapping potential  $V_{\text{ext}} = r^2$  included.

The BDG equations for condensates with short-range interaction were first solved numerically by Refs. [29,30]. In this work we used the method discussed in Sec. II B.

Figure 9 shows the eigenfrequencies of the Bogoliubov excitations of the ground state with  $l = 0, 1, 2$ , and 3 as functions of the scattering length. For  $a = 0$  one obtains the equidistant eigenfrequencies of the harmonic oscillator. When the scattering length is decreased the attractive short-range interaction acts as a perturbation and the frequencies are slightly shifted. For  $a \rightarrow a_{\text{crit}} \approx -0.0575$  the lowest  $l = 0$  mode drops to zero, marking the collapse of the condensate. The lowest mode with  $l = 1$  represents the oscillation of the center of mass of the condensate and its value is exactly that of the trapping frequency  $\omega = 2\gamma = 2$ .

For comparison in Fig. 9 we also show the results for the eigenvalues of the Jacobian matrix at the ground-state fixed point obtained in the variational ansatz using five Gaussian functions in combination with spherical harmonics (19). One recognizes that in particular the eigenvalues of the lowest modes in each angular momentum band are in excellent agreement with the eigenfrequencies of the Bogoliubov excitations. It is only close to the critical scattering length that small deviations appear. The lowest, i.e., center-of-mass excitation with  $l = 1$  can even be reproduced within numerical accuracy, independently of the number of Gaussian functions used. For the higher modes with eigenvalues of the Jacobian  $\omega > 10$ , only far away from the critical point do the variational and full-numerical results still approximately

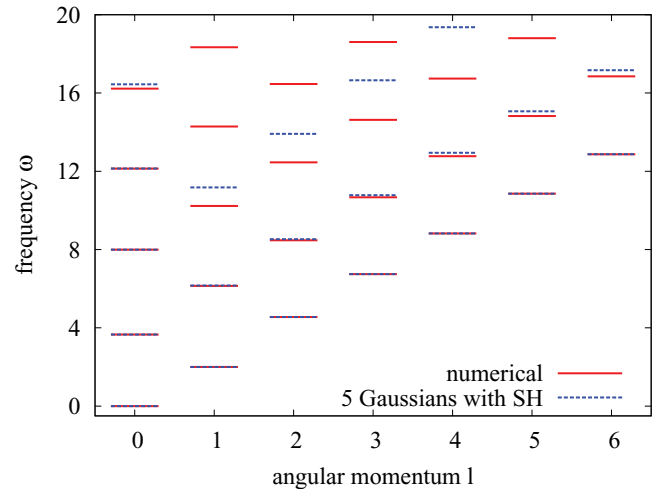


FIG. 10. (Color online) Comparison of both spectra as in Fig. 9, but here for a fixed scattering length of  $a = -0.4$  and angular momenta up to  $l = 6$ . For  $l = 0$  the variational ansatz reproduces the Bogoliubov frequencies very well for the four lowest modes and with only small deviations for the two lowest modes in the higher angular momentum bands.

correspond to each other, and in the vicinity of the critical scattering length the Jacobi eigenvalues can reproduce the behavior of the Bogoliubov excitation eigenfrequencies only qualitatively.

We also tested the variational ansatz (19) for higher angular momenta up to  $l = 6$ . The results for a fixed scattering length of  $a = -0.4$  are presented in Fig. 10. One recognizes a very good agreement for the lowest modes in each  $l$  band and small differences for the second-lowest modes. This demonstrates that for condensates with attractive short-range interaction the eigenvalues of the Jacobian matrix Eq. (26) indeed quantitatively coincide with the eigenfrequencies of the lowest Bogoliubov modes.

### C. Application of the variational approach to the monopolar condensate

We now apply the extended variational ansatz (19) to the self-trapped monopolar condensate. For the three lowest excitations Fig. 11 shows the comparison of the full-numerical Bogoliubov spectrum with the spectrum obtained from the eigenvalues of the Jacobian matrix in the variational ansatz. We used  $N = 6$  Gaussian functions and angular momenta up to  $l = 3$ . The lowest modes for  $l = 0$  and 1 match very well in the whole range of scattering lengths considered. For the second-lowest  $l = 0$  and 1 and the lowest  $l = 2$  mode we find good agreement, but the differences become larger as the scattering length approaches the critical point. Nevertheless, we have the result that the variational ansatz with coupled Gaussian functions and spherical harmonics is a valid alternative to the full-numerical quantum-mechanical approach also in this case, if one is interested in these modes.

Looking at the lowest mode with  $l = 3$ , one finds that the agreement is good for scattering lengths around  $a = 0$ , but the two frequencies deviate as the scattering length is

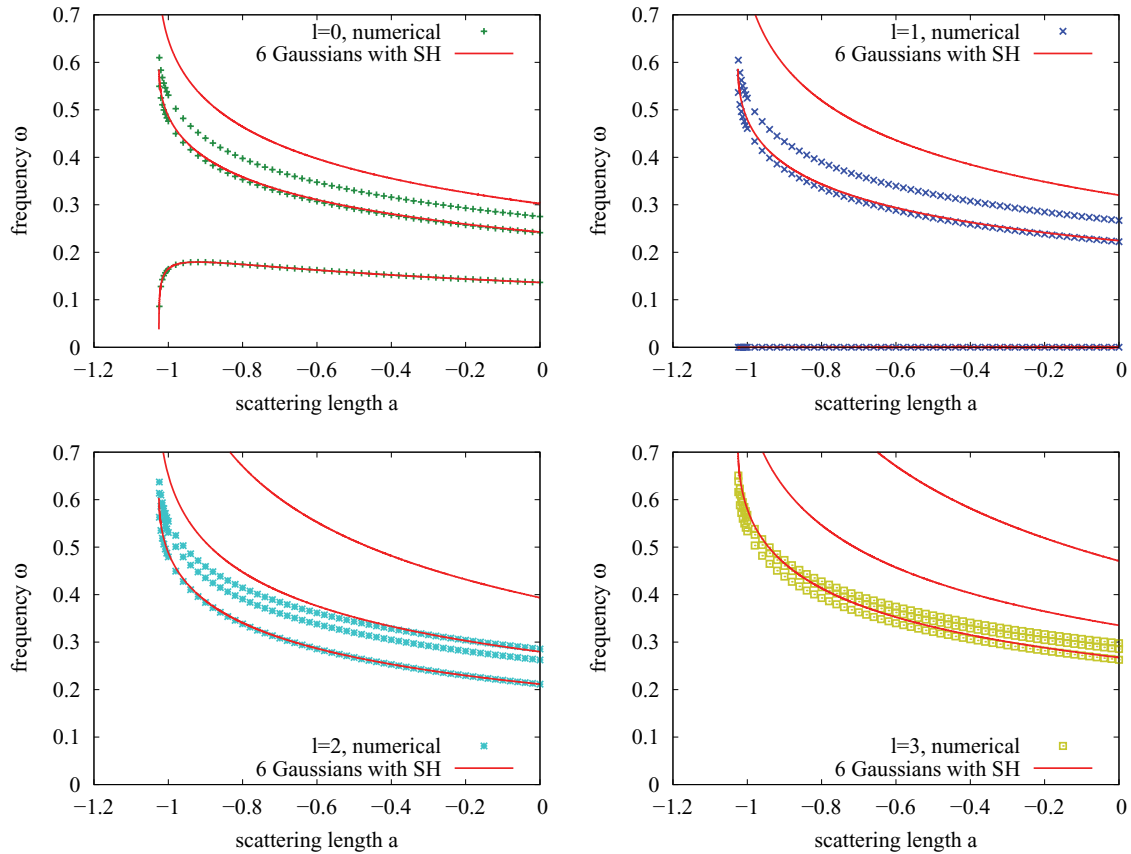


FIG. 11. (Color online) Comparison of the full-numerical Bogoliubov spectrum of the ground state of a self-trapped monopolar BEC with the spectrum obtained from the variational ansatz with coupled Gaussian functions and SH. The variational ansatz has been used with six coupled Gaussian functions and spherical harmonics up to an angular momentum of  $l = 3$ . For the lowest  $l = 0$  and 1 modes the results of both methods almost cannot be distinguished. The differences in the frequencies of the second lowest  $l = 0$  and 1 and the lowest  $l = 2$  modes are small in the range of the scattering length considered. The lowest  $l = 3$  mode is well approximated by the variational ansatz, but the differences in frequency are larger compared to the frequencies belonging to lower angular momenta. For the higher modes there is no quantitative agreement.

decreased. The eigenmode of the variational ansatz can only be seen as an approximation to the full-numerical one. The other modes can only be described qualitatively by the variational approach.

We also applied the variational ansatz (19) for higher angular momenta up to  $l = 6$ . The results for a fixed scattering length of  $a = -0.4$  are presented in Fig. 12. As already noted, only the lowest modes and angular momenta agree well with the numerically exact values. In the remaining modes the excitation frequencies differ distinctly. For  $l = 5$  the frequency of the lowest mode even lies above the negative chemical potential, which could be identified as the upper limit of the Bogoliubov spectrum. Obviously, the variational ansatz with coupled Gaussian functions and spherical harmonics is not as appropriate for the self-trapped monopolar condensate as for the condensate without long-range interaction. To obtain still better results in the variational ansatz it would be necessary to use more than  $N = 6$  coupled Gaussian functions. This, however, leads to numerical difficulties since the matrix  $\mathbf{K}$  in the equations of motion (22) becomes more and more ill-conditioned when the number of Gaussian functions is increased, which leads to an inaccurate solution of the linear system of equations.

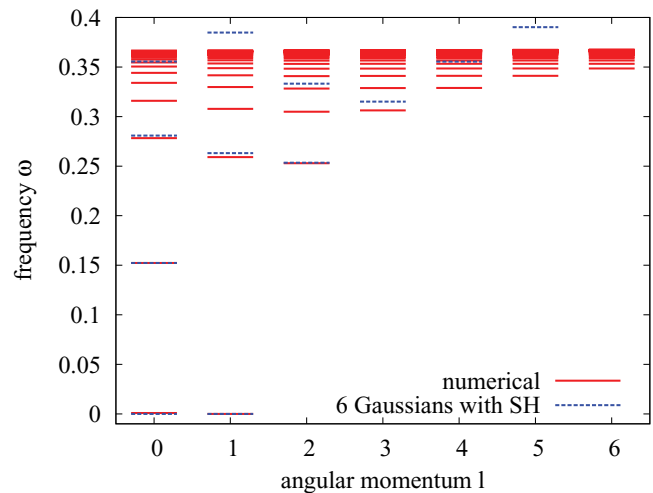


FIG. 12. (Color online) Comparison of both spectra as in Fig. 11 for a self-trapped monopolar BEC at the fixed scattering length of  $a = -0.4$  and angular momenta up to  $l = 6$ . For  $l = 0$  and 1 the two lowest modes and for  $l = 2$  and 3 only the lowest modes agree well. For higher angular momenta  $l \geq 5$  the lowest mode lies even above the limit of the numerical Bogoliubov spectrum (compare with Fig. 5).

#### IV. CONCLUSION

We have investigated the Bogoliubov spectrum of the self-trapped monopolar condensate full numerically with the finite-difference method. With this method we were able to calculate many modes for angular momenta from  $l = 0$  to 6. We found a structure similar to that in the spectra of alkali-metal atoms. The behavior could be explained by quantum-defect theory and it was found that practically the entire spectrum can be described by a simple Rydberg formula with quantum defects.

As an alternative to full-numerical calculations of condensate excitations a variational ansatz was presented that combines coupled Gaussian functions with spherical harmonics. Using the time-dependent variational principle, we could derive the equations of motion for the variational parameters. We applied the variational ansatz to two different systems. For condensates with an attractive short-range interaction we found that there is good agreement between the quantum-mechanical eigenfrequencies of the lowest Bogoliubov excitations and the eigenvalues of the Jacobian stability matrix. In this way we have been able to link the concepts of stability in quantum mechanics and in classical dynamical systems with each other.

For self-trapped condensates with additional  $1/r$  interaction we also found good agreement for the very lowest modes, but the variational ansatz works less well for higher modes. The reason for this is that for the condensate without long-range interaction in an external trap, the confining radially symmetric harmonic potential dominates the properties of the system in a wide range of the scattering length. The contact interaction seemingly acts as a perturbation. Therefore, a variational ansatz in which the radial part is determined by Gaussian functions is very well adapted to describe the stationary solutions and their excitations.

For the self-trapped monopolar condensate, in contrast, an external trap is missing and the interactions alone determine the properties of the system. As pointed out in Sec. IID, the asymptotic form for  $r \rightarrow \infty$  of the BDG equations is equivalent to the Schrödinger equation of the hydrogen atom. Therefore, in that range the solutions  $u$  and  $v$  could be approximated by Laguerre polynomials and the exponential function  $\exp(-\alpha r)$  with some  $\alpha > 0$ . A variational ansatz with coupled Gaussian functions and spherical harmonics is not well suited to reproduce this asymptotic behavior. However, as soon as a radially symmetric trap is switched on, the agreement between the quantum-mechanical and the nonlinear dynamics excitations is present again also for the higher modes.

Altogether it was shown that especially in the case without long-range interactions the extended variational ansatz works well and can reproduce the lowest modes for arbitrary angular momenta, which is significant progress compared to the ansatz with coupled Gaussian functions only. If one is interested only in the lowest modes, the ansatz is a valid alternative to the full-numerical calculations.

So far we calculated only the linear dynamics in the vicinity of a stationary solution. It remains to be shown whether or not the ansatz is capable of describing also the full-nonlinear dynamics of a BEC. Furthermore, the present ansatz is restricted to radially symmetric systems. To calculate excitations of cylindrically symmetric systems with arbitrary angular momenta, which would be necessary, e.g., for condensates

with dipole-dipole long-range interactions, an extension of the ansatz is required. For dipolar condensates such an ansatz would be of interest since the dipolar interaction offers the possibility for a condensate to collapse with  $m = 2, 3, \dots$  symmetry, the so-called angular collapse [8].

#### ACKNOWLEDGMENT

This work was supported by Deutsche Forschungsgemeinschaft.

#### APPENDIX: INTEGRALS FOR THE VARIATIONAL ANSATZ WITH COUPLED GAUSSIAN FUNCTIONS AND SPHERICAL HARMONICS

We give the integrals necessary for setting up the equations of motion resulting from the time-dependent variational principle for the variational ansatz (19). We need the matrix and vector

$$K_{ij} = \left\langle \frac{\partial \psi}{\partial z_i} \left| \frac{\partial \psi}{\partial z_j} \right. \right\rangle, \quad (\text{A1a})$$

$$h_i = \left\langle \frac{\partial \psi}{\partial z_i} \left| \hat{H} \psi \right. \right\rangle, \quad (\text{A1b})$$

where the mean-field Hamiltonian  $\hat{H}$  consists of four parts

$$\begin{aligned} \hat{H} &= \hat{T} + V_{\text{ext}} + V_s + V_m \\ &= -\Delta + \gamma_r^2 r^2 + 8\pi a |\psi(\mathbf{r})|^2 - 2 \int d^3 r' \frac{|\psi(\mathbf{r}')|^2}{|\mathbf{r} - \mathbf{r}'|}. \end{aligned} \quad (\text{A2})$$

To calculate the integrals, we write the ansatz (19) in a slightly different form

$$\psi = \sum_{k=1}^N \sum_{l,m} d_{lm}^k Y_{lm}(\theta, \phi) r^l e^{-A_r^k r^2 - \gamma^k}, \quad (\text{A3})$$

where all  $d_{00}^k \equiv 1$  have to be treated as constants and not as variational parameters.

##### 1. Integrals of the $\mathbf{K}$ matrix

For the elements of the  $\mathbf{K}$  matrix, one needs the integrals over two spherical harmonics, which because of their orthogonality are given by Kronecker  $\delta$  functions, and the integrals over the radial coordinate, which are all of the form

$$I_r = \int_0^\infty dr r^l \exp(-Ar^2). \quad (\text{A4})$$

With the substitution  $r \rightarrow t = Ar^2$ , one can use the  $\Gamma$  function [25] to write

$$I_r = \frac{1}{2} A^{-(l+1)/2} \Gamma[(l+1)/2]. \quad (\text{A5})$$

For the elements of the  $\mathbf{K}$  matrix we then obtain, with the definitions  $A_r^{kl} \equiv A_r^k + (A_r^l)^*$  and  $\gamma^{kl} \equiv \gamma^k + (\gamma^l)^*$ ,

$$\left\langle \frac{\partial \psi}{\partial d_{l_2 m_2}^l} \left| \frac{\partial \psi}{\partial d_{l_1 m_1}^k} \right. \right\rangle = \frac{1}{2} \delta_{l_1 l_2} \delta_{m_1 m_2} \frac{\Gamma(l_1 + 3/2)}{(A_r^{kl})^{l_1 + 3/2}} e^{-\gamma^{kl}}, \quad (\text{A6})$$

$$\left\langle \frac{\partial \psi}{\partial d_{l_2 m_2}^l} \left| \frac{\partial \psi}{\partial A_r^k} \right. \right\rangle = -\frac{1}{2} d_{l_2 m_2}^k \frac{\Gamma(l_2 + 5/2)}{(A_r^{kl})^{l_2 + 5/2}} e^{-\gamma^{kl}}, \quad (\text{A7})$$

$$\left\langle \frac{\partial \psi}{\partial d_{l_2 m_2}^l} \left| \frac{\partial \psi}{\partial \gamma^k} \right. \right\rangle = -\frac{1}{2} d_{l_2 m_2}^k \frac{\Gamma(l_2 + 3/2)}{(A_r^{kl})^{l_2 + 3/2}} e^{-\gamma^{kl}}, \quad (\text{A8})$$

$$\left\langle \frac{\partial \psi}{\partial A_r^l} \left| \frac{\partial \psi}{\partial A_r^k} \right. \right\rangle = \frac{1}{2} \sum_{l_1, m_1} (d_{l_1 m_1}^l)^* d_{l_1 m_1}^k \frac{\Gamma(l_1 + 7/2)}{(A_r^{kl})^{l_1 + 7/2}} e^{-\gamma^{kl}}, \quad (\text{A9})$$

$$\left\langle \frac{\partial \psi}{\partial A_r^l} \left| \frac{\partial \psi}{\partial \gamma^k} \right. \right\rangle = \frac{1}{2} \sum_{l_1, m_1} (d_{l_1 m_1}^l)^* d_{l_1 m_1}^k \frac{\Gamma(l_1 + 5/2)}{(A_r^{kl})^{l_1 + 5/2}} e^{-\gamma^{kl}}, \quad (\text{A10})$$

$$\left\langle \frac{\partial \psi}{\partial \gamma^l} \left| \frac{\partial \psi}{\partial \gamma^k} \right. \right\rangle = \frac{1}{2} \sum_{l_1, m_1} (d_{l_1 m_1}^l)^* d_{l_1 m_1}^k \frac{\Gamma(l_1 + 3/2)}{(A_r^{kl})^{l_1 + 3/2}} e^{-\gamma^{kl}}. \quad (\text{A11})$$

## 2. Integrals of the kinetic term

For the calculation of the integrals of the kinetic term, one lets the Laplacian act on the variational ansatz. The integrals of the resulting terms can then be evaluated using Eq. (A5), which leads to

$$\left\langle \frac{\partial \psi}{\partial d_{l_2 m_2}^l} \left| \hat{T} \psi \right. \right\rangle = \frac{1}{2} \sum_{k=1}^N d_{l_2 m_2}^k \left[ (4l_2 + 6) A_r^k \frac{\Gamma(l_2 + 3/2)}{(A_r^k)^{l_2 + 3/2}} - 4(A_r^k)^2 \frac{\Gamma(l_2 + 5/2)}{(A_r^k)^{l_2 + 5/2}} \right] e^{-\gamma^{kl}}, \quad (\text{A12})$$

$$\left\langle \frac{\partial \psi}{\partial A_r^l} \left| \hat{T} \psi \right. \right\rangle = -\frac{1}{2} \sum_{k=1}^N \sum_{l_1, m_1} (d_{l_1 m_1}^l)^* d_{l_1 m_1}^k \left[ (4l_1 + 6) A_r^k \frac{\Gamma(l_1 + 5/2)}{(A_r^{kl})^{l_1 + 5/2}} - 4(A_r^k)^2 \frac{\Gamma(l_1 + 7/2)}{(A_r^{kl})^{l_1 + 7/2}} \right] e^{-\gamma^{kl}}, \quad (\text{A13})$$

$$\left\langle \frac{\partial \psi}{\partial \gamma^l} \left| \hat{T} \psi \right. \right\rangle = -\frac{1}{2} \sum_{k=1}^N \sum_{l_1, m_1} (d_{l_1 m_1}^l)^* d_{l_1 m_1}^k \left[ (4l_1 + 6) A_r^k \frac{\Gamma(l_1 + 3/2)}{(A_r^{kl})^{l_1 + 3/2}} - 4(A_r^k)^2 \frac{\Gamma(l_1 + 5/2)}{(A_r^{kl})^{l_1 + 5/2}} \right] e^{-\gamma^{kl}}. \quad (\text{A14})$$

## 3. Integrals of the trapping potential

The integrals for the trapping potential are straightforward:

$$\left\langle \frac{\partial \psi}{\partial d_{l_2 m_2}^l} \left| V_{\text{ext}} \psi \right. \right\rangle = \frac{1}{2} \gamma_r^2 \sum_{k=1}^N d_{l_2 m_2}^k \frac{\Gamma(l_2 + 5/2)}{(A_r^k)^{l_2 + 5/2}} e^{-\gamma^{kl}}, \quad (\text{A15})$$

$$\left\langle \frac{\partial \psi}{\partial A_r^l} \left| V_{\text{ext}} \psi \right. \right\rangle = -\frac{1}{2} \gamma_r^2 \sum_{k=1}^N \sum_{l_1, m_1} (d_{l_1 m_1}^l)^* d_{l_1 m_1}^k \times \frac{\Gamma(l_1 + 7/2)}{(A_r^{kl})^{l_1 + 7/2}} e^{-\gamma^{kl}}, \quad (\text{A16})$$

$$\left\langle \frac{\partial \psi}{\partial \gamma^l} \left| V_{\text{ext}} \psi \right. \right\rangle = -\frac{1}{2} \gamma_r^2 \sum_{k=1}^N \sum_{l_1, m_1} (d_{l_1 m_1}^l)^* d_{l_1 m_1}^k \times \frac{\Gamma(l_1 + 5/2)}{(A_r^{kl})^{l_1 + 5/2}} e^{-\gamma^{kl}}. \quad (\text{A17})$$

## 4. Integrals of the scattering term

To write the integrals of the scattering term we introduce the abbreviations  $A_r^{ijkl} = A_r^{ij} + A_r^{kl}$  and  $\gamma^{ijkl} = \gamma^{ij} + \gamma^{kl}$  and for the integral over four spherical harmonics the notation

$$I_{\Omega}^{(4)}(l_1, m_1; l_2, m_2; l_3, m_3; l_4, m_4) = \int d\Omega Y_{l_1 m_1}(\theta, \phi) Y_{l_2 m_2}(\theta, \phi) Y_{l_3 m_3}(\theta, \phi) Y_{l_4 m_4}(\theta, \phi), \quad (\text{A18})$$

where  $d\Omega = d\phi d\theta \sin\theta$  is the differential solid angle element of the angular coordinates. Using again Eq. (A5), we obtain for the integrals

$$\left\langle \frac{\partial \psi}{\partial d_{l_2 m_2}^l} \left| V_s \psi \right. \right\rangle = 4\pi a \sum_{i, j, k=1}^N \sum_{l_1, m_1} \sum_{l_3, m_3} \sum_{l_4, m_4} (-1)^{m_2 + m_4} (d_{l_4 m_4}^j)^* d_{l_3 m_3}^i d_{l_1 m_1}^k \times \frac{\Gamma[(l_1 + l_2 + l_3 + l_4 + 3)/2]}{(A_r^{ijkl})^{-(l_1 + l_2 + l_3 + l_4 + 3)/2}} I_{\Omega}^{(4)}(l_2, -m_2; l_4, -m_4; l_3, m_3; l_1, m_1) e^{-\gamma^{ijkl}}, \quad (\text{A19})$$

$$\left\langle \frac{\partial \psi}{\partial A_r^l} \left| V_s \psi \right. \right\rangle = -4\pi a \sum_{i, j, k=1}^N \sum_{l_1, m_1} \sum_{l_2, m_2} \sum_{l_3, m_3} \sum_{l_4, m_4} (-1)^{m_2 + m_4} (d_{l_2 m_2}^l)^* (d_{l_4 m_4}^j)^* d_{l_3 m_3}^i d_{l_1 m_1}^k \times \frac{\Gamma[(l_1 + l_2 + l_3 + l_4 + 5)/2]}{(A_r^{ijkl})^{-(l_1 + l_2 + l_3 + l_4 + 5)/2}} I_{\Omega}^{(4)}(l_2, -m_2; l_4, -m_4; l_3, m_3; l_1, m_1) e^{-\gamma^{ijkl}}, \quad (\text{A20})$$

$$\left\langle \frac{\partial \psi}{\partial \gamma^l} \left| V_s \psi \right. \right\rangle = -4\pi a \sum_{i, j, k=1}^N \sum_{l_1, m_1} \sum_{l_2, m_2} \sum_{l_3, m_3} \sum_{l_4, m_4} (-1)^{m_2 + m_4} (d_{l_2 m_2}^l)^* (d_{l_4 m_4}^j)^* d_{l_3 m_3}^i d_{l_1 m_1}^k \times \frac{\Gamma[(l_1 + l_2 + l_3 + l_4 + 3)/2]}{(A_r^{ijkl})^{-(l_1 + l_2 + l_3 + l_4 + 3)/2}} I_{\Omega}^{(4)}(l_2, -m_2; l_4, -m_4; l_3, m_3; l_1, m_1) e^{-\gamma^{ijkl}}. \quad (\text{A21})$$

An analytical expression for  $I_{\Omega}^{(4)}$  is found by noting that the product of two spherical harmonics can be expressed by a series of spherical harmonics

$$Y_{l_1 m_1}(\theta, \phi) Y_{l_2 m_2}(\theta, \phi) = \sum_{l=0}^{\infty} \sum_{m=-l}^l C_{l \ l_1 \ l_2}^{m \ m_1 \ m_2} Y_{lm}(\theta, \phi), \quad (\text{A22})$$

where the coefficients  $C_{l \ l_1 \ l_2}^{m \ m_1 \ m_2}$  can be written in terms of Wigner 3- $j$  symbols [31]

$$C_{l \ l_1 \ l_2}^{m \ m_1 \ m_2} = (-1)^m \sqrt{\frac{(2l_1 + 1)(2l_2 + 1)(2l + 1)}{4\pi}} \times \begin{pmatrix} l_1 & l_2 & l \\ 0 & 0 & 0 \end{pmatrix} \begin{pmatrix} l_1 & l_2 & l \\ m_1 & m_2 & -m \end{pmatrix}. \quad (\text{A23})$$

Applying this expansion twice in the integral Eq. (A18), we obtain

$$I_{\Omega}^{(4)}(l_1, m_1; l_2, m_2; l_3, m_3; l_4, m_4) = \sum_{l=0}^{\infty} \sum_{m=-l}^l (-1)^m C_{l \ l_1 \ l_2}^{m \ m_1 \ m_2} C_{l \ l_3 \ l_4}^{-m \ m_3 \ m_4}. \quad (\text{A24})$$

The infinite sum can be cut off since a Wigner 3- $j$  symbol is zero if the triangle inequalities  $|l_1 - l_2| \leq l \leq l_1 + l_2$  or  $|l_3 - l_4| \leq l \leq l_3 + l_4$  are not fulfilled and  $l_1, \dots, l_4$  cannot be greater than the largest angular momentum included in the variational ansatz.

### 5. Integrals of the monopolar term

The integrals for the monopolar term read

$$\left\langle \frac{\partial \psi}{\partial d_{l_2 m_2}^l} \middle| V_m \psi \right\rangle = -2 \sum_{i,j,k=1}^N \sum_{l_1, m_1} \sum_{l_2, m_2} \sum_{l_3, m_3} \sum_{l_4, m_4} (d_{l_4 m_4}^j)^* d_{l_3 m_3}^i d_{l_1 m_1}^k I_{m,0}, \quad (\text{A25})$$

$$\left\langle \frac{\partial \psi}{\partial A_r^l} \middle| V_m \psi \right\rangle = 2 \sum_{i,j,k=1}^N \sum_{l_1, m_1} \sum_{l_2, m_2} \sum_{l_3, m_3} \sum_{l_4, m_4} (d_{l_2 m_2}^l)^* (d_{l_4 m_4}^j)^* \times d_{l_3 m_3}^i d_{l_1 m_1}^k I_{m,2}, \quad (\text{A26})$$

$$\left\langle \frac{\partial \psi}{\partial \gamma^l} \middle| V_m \psi \right\rangle = 2 \sum_{i,j,k=1}^N \sum_{l_1, m_1} \sum_{l_2, m_2} \sum_{l_3, m_3} \sum_{l_4, m_4} (d_{l_2 m_2}^l)^* (d_{l_4 m_4}^j)^* \times d_{l_3 m_3}^i d_{l_1 m_1}^k I_{m,0}, \quad (\text{A27})$$

with the definition

$$I_{m,p} = \int d\Omega \int_0^{\infty} dr \int d\Omega' \int_0^{\infty} dr' \frac{1}{|\mathbf{r} - \mathbf{r}'|} \times Y_{l_2 m_2}^*(\theta, \phi) Y_{l_1 m_1}(\theta, \phi) Y_{l_4 m_4}^*(\theta', \phi') Y_{l_3 m_3}(\theta', \phi') \times r^{l_1 + l_2 + p + 2} (r')^{l_3 + l_4 + 2} e^{-A_r^{kl} r^2} e^{-A_r^{ij} (r')^2}. \quad (\text{A28})$$

To calculate this integral, the monopolar interaction potential  $1/|\mathbf{r} - \mathbf{r}'|$  is expanded in terms of multipoles [25]

$$\frac{1}{|\mathbf{r} - \mathbf{r}'|} = \sum_{l=0}^{\infty} \sum_{m=-l}^l \frac{4\pi}{2l+1} \frac{r_{<}^l}{r_{>}^{l+1}} Y_{lm}^*(\theta, \phi) Y_{lm}(\theta', \phi'). \quad (\text{A29})$$

The integral  $I_{m,p}$  then separates into two integrals over the angular coordinates  $\Omega$  and  $\Omega'$ , which can be expressed with the coefficients  $C_{l \ l_1 \ l_2}^{m \ m_1 \ m_2}$  from Eq. (A23), and one integral over the radial coordinates  $r$  and  $r'$ , which is of Gaussian type and can be solved analytically. For  $I_{m,p}$  we obtain

$$I_{m,p} = \sum_{l=0}^{\infty} \sum_{m=-l}^l \frac{4\pi}{2l+1} I_m^{\Omega} I_m^{\Omega'} I_{m,p}^{r,r'}, \quad (\text{A30})$$

with the individual integrals

$$I_m^{\Omega} = (-1)^m C_{l_2 \ l_1 \ l}^{m_2 \ m_1 \ m}, \quad (\text{A31})$$

$$I_m^{\Omega'} = C_{l_4 \ l_3 \ l}^{m_4 \ m_3 \ m}, \quad (\text{A32})$$

and

$$I_{m,p}^{r,r'} = \frac{1}{4} \frac{[(l_3 + l_4 - l)/2]!}{(A_r^{ij})^{(l_3 + l_4 - l + 2)/2} (A_r^{ijkl})^{(l_1 + l_2 + l + p + 3)/2}} \sum_{\alpha=0}^{(l_3 + l_4 - l)/2} \times \frac{1}{\alpha!} \left( \frac{A_r^{ij}}{A_r^{ijkl}} \right)^{\alpha} \Gamma[(l_1 + l_2 + l + p + 2\alpha + 3)/2] + \frac{1}{4} \frac{[(l_1 + l_2 - l + p)/2]!}{(A_r^{kl})^{(l_1 + l_2 - l + p + 2)/2} (A_r^{ijkl})^{(l_3 + l_4 + l + 3)/2}} \sum_{\alpha=0}^{(l_1 + l_2 - l + p)/2} \times \frac{1}{\alpha!} \left( \frac{A_r^{kl}}{A_r^{ijkl}} \right)^{\alpha} \Gamma[(l_3 + l_4 + l + 2\alpha + 3)/2]. \quad (\text{A33})$$

The infinite sum in Eq. (A30) can be cut off again due to the properties of the Wigner 3- $j$  symbols. Thus all integrals necessary for setting up the equations of motion for the variational parameters for the ansatz with coupled Gaussian functions and spherical harmonics have been calculated analytically.

[1] S. Rau, J. Main, and G. Wunner, *Phys. Rev. A* **82**, 023610 (2010).  
 [2] S. Rau, J. Main, H. Cartarius, P. Köberle, and G. Wunner, *Phys. Rev. A* **82**, 023611 (2010).  
 [3] A. Griesmaier, J. Werner, S. Hensler, J. Stuhler, and T. Pfau, *Phys. Rev. Lett.* **94**, 160401 (2005).  
 [4] J. Stuhler, A. Griesmaier, T. Koch, M. Fattori, T. Pfau, S. Giovanazzi, P. Pedri, and L. Santos, *Phys. Rev. Lett.* **95**, 150406 (2005).  
 [5] L. Santos, G. V. Shlyapnikov, and M. Lewenstein, *Phys. Rev. Lett.* **90**, 250403 (2003).

[6] S. Ronen, D. C. E. Bortolotti, and J. L. Bohn, *Phys. Rev. Lett.* **98**, 030406 (2007).  
 [7] O. Dutta and P. Meystre, *Phys. Rev. A* **75**, 053604 (2007).  
 [8] R. M. Wilson, S. Ronen, and J. L. Bohn, *Phys. Rev. A* **80**, 023614 (2009).  
 [9] M. Lu, S. H. Youn, and B. L. Lev, *Phys. Rev. Lett.* **104**, 063001 (2010).  
 [10] M. Lu, N. Q. Burdick, S. H. Youn, and B. L. Lev, *Phys. Rev. Lett.* **107**, 190401 (2011).

- [11] J. J. McClelland and J. L. Hanssen, *Phys. Rev. Lett.* **96**, 143005 (2006).
- [12] D. O'Dell, S. Giovanazzi, G. Kurizki, and V. M. Akulin, *Phys. Rev. Lett.* **84**, 5687 (2000).
- [13] I. Papadopoulos, P. Wagner, G. Wunner, and J. Main, *Phys. Rev. A* **76**, 053604 (2007).
- [14] S. Giovanazzi, G. Kurizki, I. E. Mazets, and S. Stringari, *Europhys. Lett.* **56**, 1 (2001).
- [15] H. Cartarius, T. Fabčić, J. Main, and G. Wunner, *Phys. Rev. A* **78**, 013615 (2008).
- [16] V. M. Pérez-García, H. Michinel, J. I. Cirac, M. Lewenstein, and P. Zoller, *Phys. Rev. Lett.* **77**, 5320 (1996).
- [17] E. J. Heller, *J. Chem. Phys.* **65**, 4979 (1976).
- [18] E. J. Heller, *J. Chem. Phys.* **75**, 2923 (1981).
- [19] D. Buccoliero, A. S. Desyatnikov, W. Krolikowski, and Y. S. Kivshar, *Phys. Rev. Lett.* **98**, 053901 (2007).
- [20] D. Buccoliero and A. S. Desyatnikov, *Opt. Express* **17**, 9608 (2009).
- [21] F. Maucher, S. Skupin, M. Shen, and W. Krolikowski, *Phys. Rev. A* **81**, 063617 (2010).
- [22] H. Cartarius, J. Main, and G. Wunner, *Phys. Rev. A* **77**, 013618 (2008).
- [23] M. J. D. Powell, in *Numerical Methods for Nonlinear Algebraic Equations*, edited by P. Rabinowitz (Gordon and Breach, London, 1970), pp. 87–114.
- [24] L. P. Pitaevskii and S. Stringari, *Bose-Einstein Condensation* (Oxford University Press, Oxford, 2003).
- [25] G. B. Arfken and H. J. Weber, *Mathematical Methods for Physicists*, 5th ed. (Academic, New York, 2001).
- [26] M. J. Seaton, *Rep. Prog. Phys.* **46**, 167 (1983).
- [27] A. D. McLachlan, *Mol. Phys.* **8**, 39 (1964).
- [28] P. A. M. Dirac, *Math. Proc. Cambridge* **26**, 376 (1930).
- [29] M. Edwards, P. A. Ruprecht, K. Burnett, R. J. Dodd, and C. W. Clark, *Phys. Rev. Lett.* **77**, 1671 (1996).
- [30] P. A. Ruprecht, M. Edwards, K. Burnett, and C. W. Clark, *Phys. Rev. A* **54**, 4178 (1996).
- [31] W. J. Thompson, *Angular Momentum: An Illustrated Guide to Rotational Symmetries for Physical Systems* (Wiley, New York, 1994).